

Supporting Information

Ni₃S₂ Nanosheets Shelled with NiFe (oxy)hydroxides as Electrocatalysts for Water Oxidation

Yu Wei,^{a#} Zhao Liu,^{b#} Taolue Liu,^a Xin Ding,^{c*} and Yan Gao^{a*}

^a State Key Laboratory of Fine Chemicals, Frontier Science Center for Smart Materials, School of Chemical Engineering, Dalian University of Technology, Dalian 116024, China. E-mail: dr.gaoyan@dlut.edu.cn

^b National Marine Environmental Monitoring Center, Ministry of Ecological Environment, Dalian 116023, China

^c College of Chemistry and Chemical Engineering, Qingdao University, Qingdao, 266071, Shandong, China. E-mail: dingxin@qdu.edu.cn

[#] *These authors contributed equally to this work*

Experimental

1. General materials

Nickel nitrate hexahydrate [$\text{Ni}(\text{NO}_3)_2 \cdot 6\text{H}_2\text{O}$, 98%] and Potassium persulfate ($\text{K}_2\text{S}_2\text{O}_8$, 99%) were purchased from Innochem chemical company. Iron perchlorate hydrate [$\text{Fe}(\text{ClO}_4)_2 \cdot x\text{H}_2\text{O}$], Sodium sulfide nonahydrate ($\text{Na}_2\text{S} \cdot 9\text{H}_2\text{O}$, 99.99%), Urea (99.5%), Ammonium fluoride (NH_4F , 98%), Acetonitrile (99.5%) and Potassium hydroxide (KOH , 95%) were purchased from Aladdin chemical company. And nickel foam (NF) was purchased from kunshan GuangJiaYuan new materials Co. Ltd (1.5 mm). Deionized water (18 $\text{M}\Omega \cdot \text{cm}^{-1}$ resistivity) was used for the preparation of all aqueous solutions. Other materials come from industrial-grade products.

2. Fabrication of the electrodes

Treatment of foamed nickel (NF). NF was cut into $2 \times 3 \text{ cm}^2$, and ethanol and acetone were respectively sonicated for 15 min to remove surface organics. After drying, sonicated with 3 M hydrochloric acid solution for 15 min to remove the surface oxide film, then washed with water for subsequent use.

Fabrication of $\text{Ni}_3\text{S}_2/\text{NF}$ electrode. To 50 mL of Teflon-lined stainless autoclave, 28 mL of H_2O , 0.144 g of NH_4F , 0.6 g of urea and 2 mL of 1 M aqueous $\text{Ni}(\text{NO}_3)_2$ were added and the solution was stirred for 10 minutes to mix thoroughly. The treated NF was then immersed in the solution mixture. The autoclave was sealed and maintained at 120 °C for 24 h. The resulting $\text{Ni}(\text{OH})_2/\text{NF}$ was dark green and was washed with water, then immersed in 30 mL of aqueous solution containing 1.44 g of $\text{Na}_2\text{S} \cdot 9\text{H}_2\text{O}$ with 50 mL Teflon-lined stainless autoclave for sulfation. The autoclave was sealed and maintained at 100 °C for 8 h. The black electrode was rinsed with a large amount of water and ethanol in turn, dried at room temperature and then $\text{Ni}_3\text{S}_2/\text{NF}$ was prepared.

Fabrication of $\text{NiFe}(\text{OH})_x/\text{Ni}_3\text{S}_2/\text{NF}$ electrode. The deposition of $\text{NiFe}(\text{OH})_x$ was accomplished by chemical method. First, the electrodes were immersed in 40 mL of aqueous solution containing 1.6 g NaOH and 0.54 g $\text{K}_2\text{S}_2\text{O}_8$ overnight. The oxidized surface of the electrode was rinsed twice with water to remove the residual solute, and

then washed once with a small amount of acetone to facilitate rapid drying at room temperature. The electrode was placed at room temperature for 10 min, then immersed in 30 mL of acetonitrile solution containing 120 mg of $\text{Fe}(\text{ClO}_4)_2 \cdot x\text{H}_2\text{O}$ and placed at room temperature for 6 h. The electrode was washed with water and dried naturally to produce the target electrode of $\text{NiFe}(\text{OH})_x/\text{Ni}_3\text{S}_2/\text{NF}$.

Fabrication of $\text{NiFe}(\text{OH})_x/\text{Ni}(\text{OH})_2/\text{NF}$ electrode. The $\text{NiFe}(\text{OH})_x/\text{Ni}(\text{OH})_2/\text{NF}$ electrode was prepared as $\text{NiFe}(\text{OH})_x/\text{Ni}_3\text{S}_2/\text{NF}$, except that there was no step of sulfation reaction.

3. Material characterization

The morphology and dimension of as-prepared materials were characterized by Nova NanoSEM 450 equipment. The microstructures of the samples were characterized by TEM (FEI TF30). X-ray diffraction (XRD) pattern was collected by a D/max-2400 diffractometer (Japan Rigaku Rotaflex) using $\text{Cu K}\alpha$ radiation ($\lambda = 154.1 \text{ nm}$). X-ray photoelectron spectroscopy (XPS) measurement was performed on a Thermo ESCALAB XI+ instrument. The binding energy (BE) was calibrated with respect to the C 1s level (284.8 eV) of adventitious carbon. Raman Spectrometer (Thermo Fisher DXR Microscope) for Analysis of Molecular Structures. Inductive Coupled Plasma Emission Spectrometer (ICP) of perkinelmer Optima2000DV was applied for the calibration of metal element content.

4. Electrochemical measurements

All the electrochemical measurements were performed by CHI 660E Electrochemical Analyzer (Shanghai Chenhua Instrument Co., Ltd) using a three-electrode system at room temperature. A 1 cm^2 of NF decorated with catalyst was used as working electrode, Pt net and HgO/Hg electrode were used as counter and reference electrodes, respectively. The electrolyte was 1M KOH solution ($\text{pH} = 13.6$). All the potentials were converted to reversible hydrogen electrode (RHE) scale, $E_{\text{RHE}} = E_{\text{HgO}/\text{Hg}} + 0.059\text{pH} + 0.106 \text{ V}$.

Before measurements, the working electrode was electrochemically activated at constant current densities of 50 mA cm^{-2} for 10 min. Linear sweep voltammetry (LSV) curves corrected with iR -compensation were tested at a scan rate of 1 mV/s . The

chronopotentiometry curve was obtained at constant current densities of 100 mA cm⁻² without iR-compensation. Tafel slopes were calculated by plotting overpotential against log (current density) with iR drop compensation. The electrochemical impedance spectroscopy (EIS) was recorded at the overpotential of 220 mV at the amplitude of the sinusoidal voltage of 5 mV over a frequency range from 0.01 Hz to 100 Hz. Cyclic voltammetry (CV) curves were collected at different scan rates in a non-Faradic region to evaluate the double-layer capacitance values (C_{dl}).

$$C_{dl} = i_c / \nu \quad \text{Equation S1}$$

$$ECSA = C_{dl} / C_s \quad \text{Equation S2}$$

Where i_c represents the charging current, ν is the scan rate, C_s is the specific capacitance

(0.040 mF/cm²), S is the geometric area of the electrode (1 cm²).

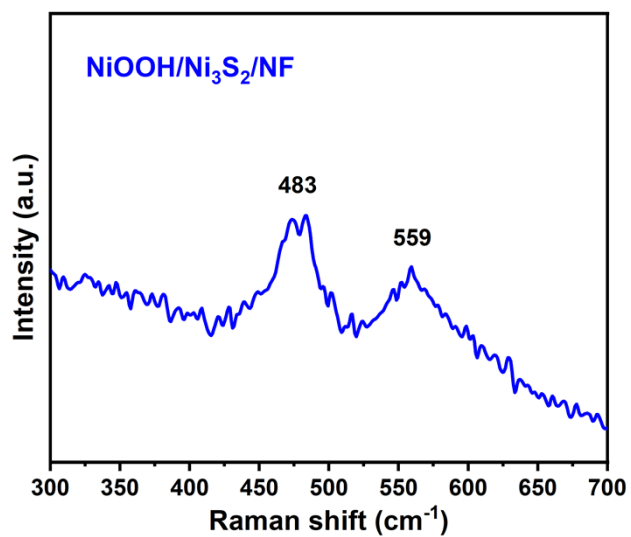


Figure S1. Raman spectrum of Ni₃S₂/NF electrode after the surface was oxidized.

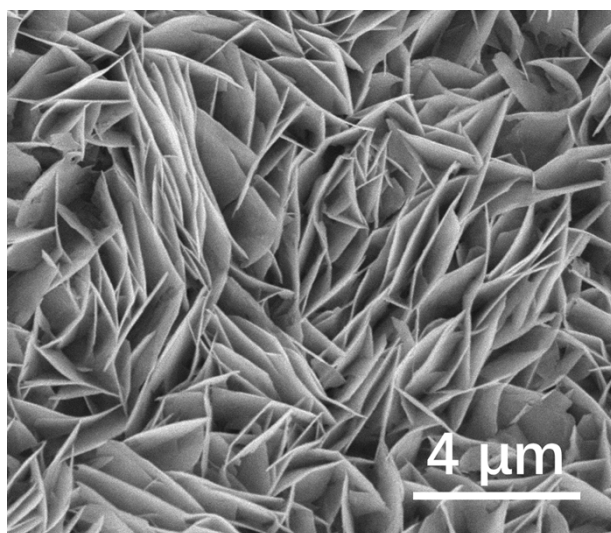


Figure S2. SEM image of the NiFe(OH)_x/Ni(OH)₂/NF

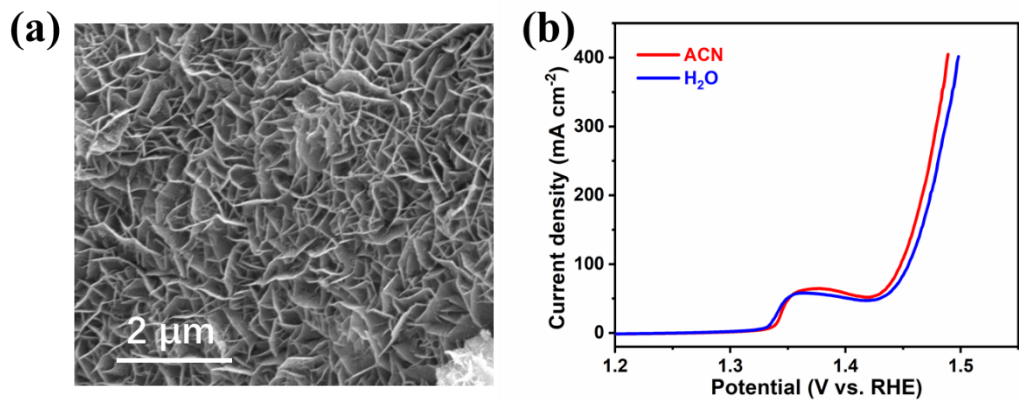


Figure S3. (a) SEM image and (b) LSV curve of electrode fabricated in water deposition solvent.

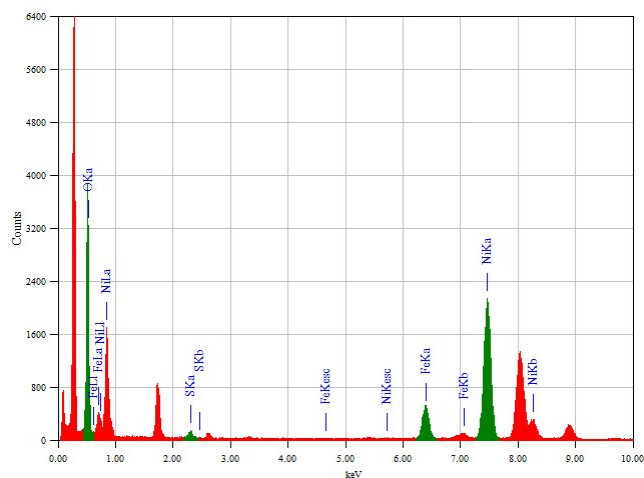


Figure S4. EDS spectra of the $\text{NiFe(OH)}_x/\text{Ni}_3\text{S}_2$.

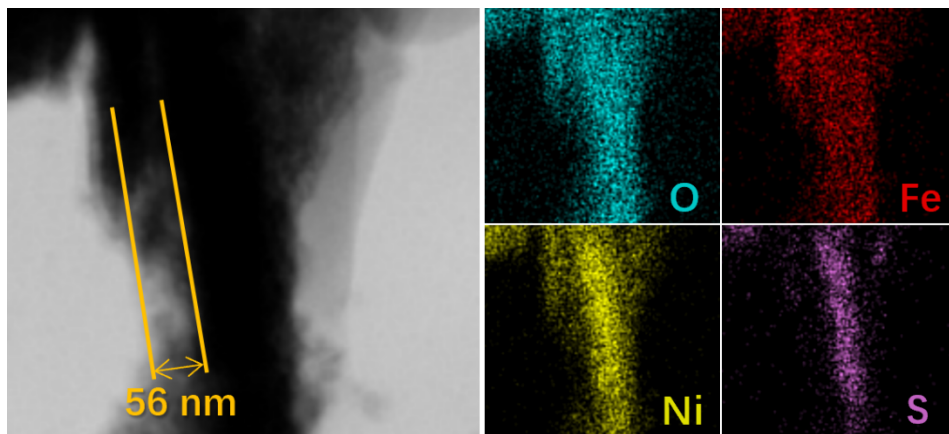


Figure S5. TEM image of $\text{NiFe(OH)}_x/\text{Ni}_3\text{S}_2$ with the corresponding elemental mapping.

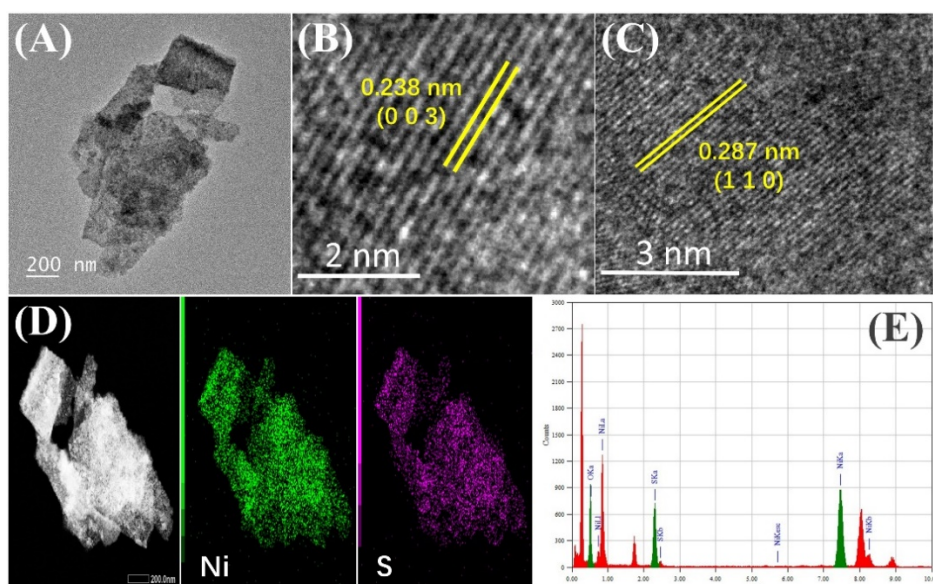


Figure S6. (A) TEM image of Ni_3S_2 . (B and C) HRTEM image of Ni_3S_2 to show the lattice fringe. (D) EDS mapping of Ni_3S_2 . (E) EDS spectra of the Ni_3S_2 .

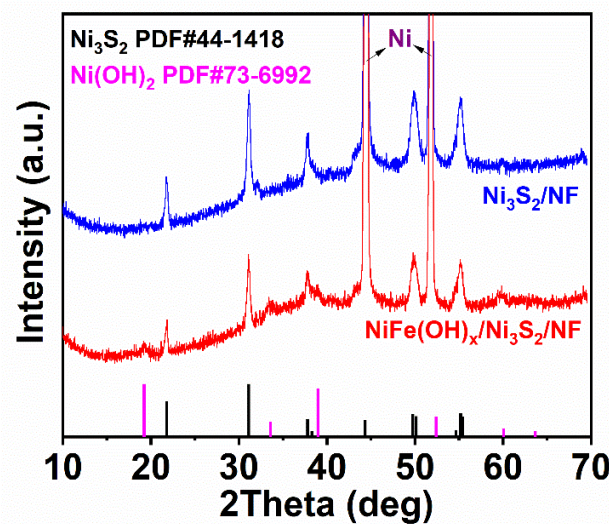


Figure S7. XRD patterns of $\text{Ni}_3\text{S}_2/\text{NF}$ and $\text{NiFe}(\text{OH})_x/\text{Ni}_3\text{S}_2/\text{NF}$.

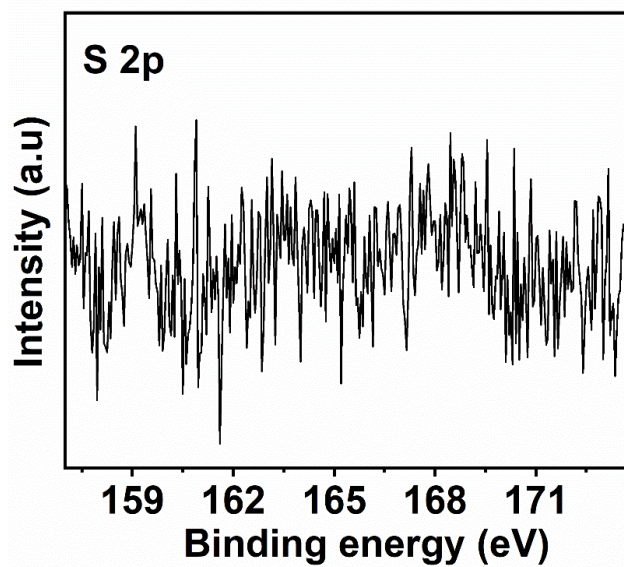


Figure S8. High-resolution X-ray photoelectron spectroscopy (XPS) spectra for the S 2p.

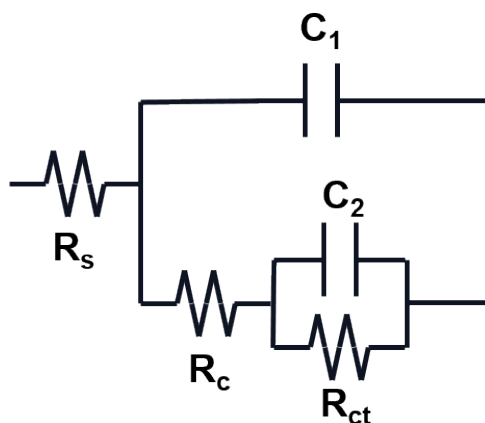


Figure S9. The equivalent circuit diagrams of electrodes. wherein R_s , R_c , and R_{ct} represent solution resistance, contact resistance, and charge-transfer resistance, respectively.

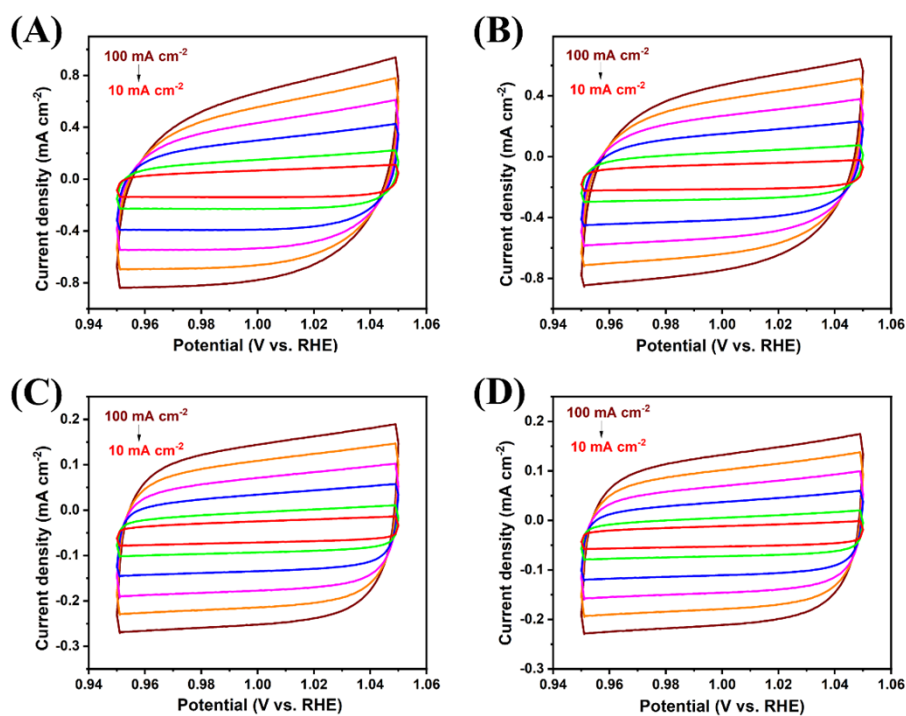


Figure S10. Typical cyclic voltammetry curves of (a) $\text{NiFe(OH)}_x/\text{Ni}_3\text{S}_2/\text{NF}$, (b) $\text{Ni}_3\text{S}_2/\text{NF}$, (c) $\text{NiFe(OH)}_x/\text{Ni(OH)}_2/\text{NF}$, and (d) $\text{Ni(OH)}_2/\text{NF}$ in 1 M KOH with different scan rates of 10, 20, 40, 60, 80, and 100 mV/s.

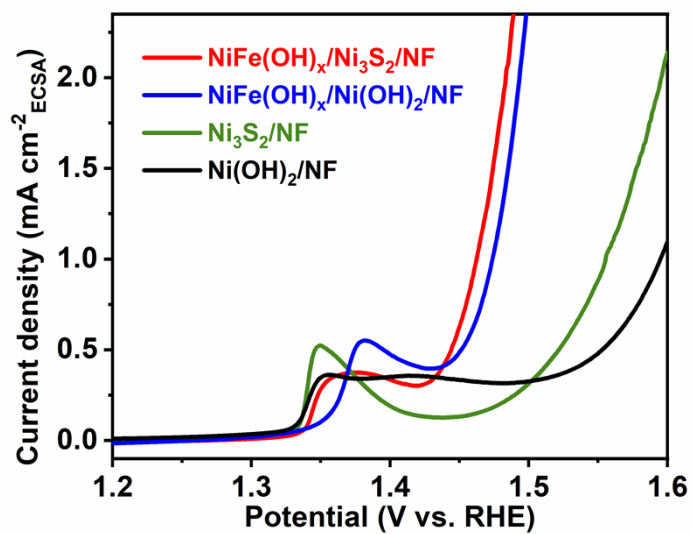


Figure S11. ECSA-normalized LSV curves of the electrodes.

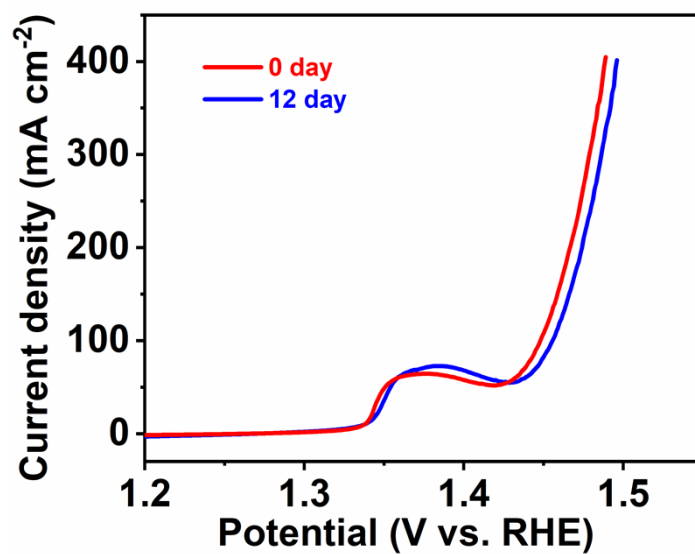


Figure S12. Polarization curves of $\text{NiFe(OH)}_x/\text{Ni}_3\text{S}_2/\text{NF}$ before and after 12 days of constant current measurement.

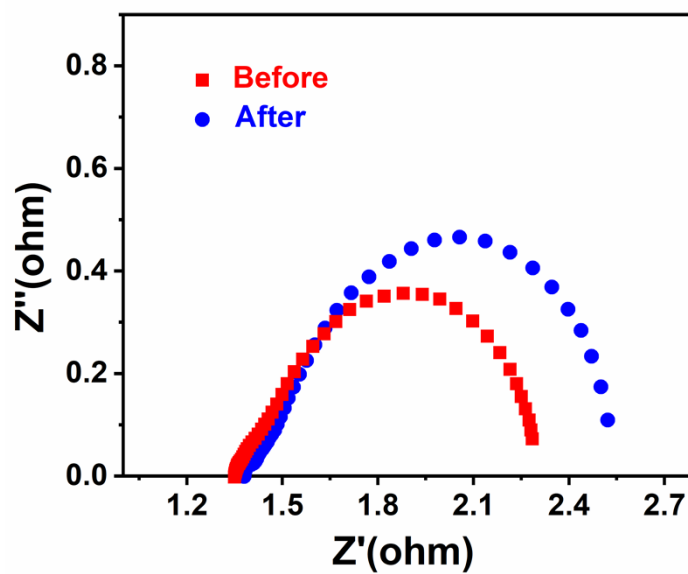


Figure S13. Nyquist plots before and after electrolysis (overpotential = 220 mV).

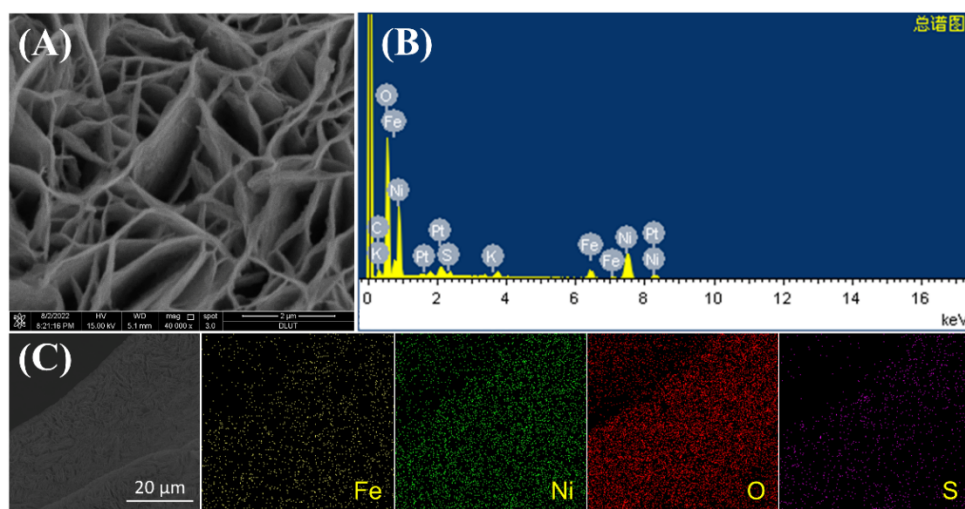


Figure S14. (A) SEM image, (B) EDS pattern and (C) Elemental mappings of the $\text{NiFe(OH)}_x/\text{Ni}_3\text{S}_2/\text{NF}$ after electrolysis.

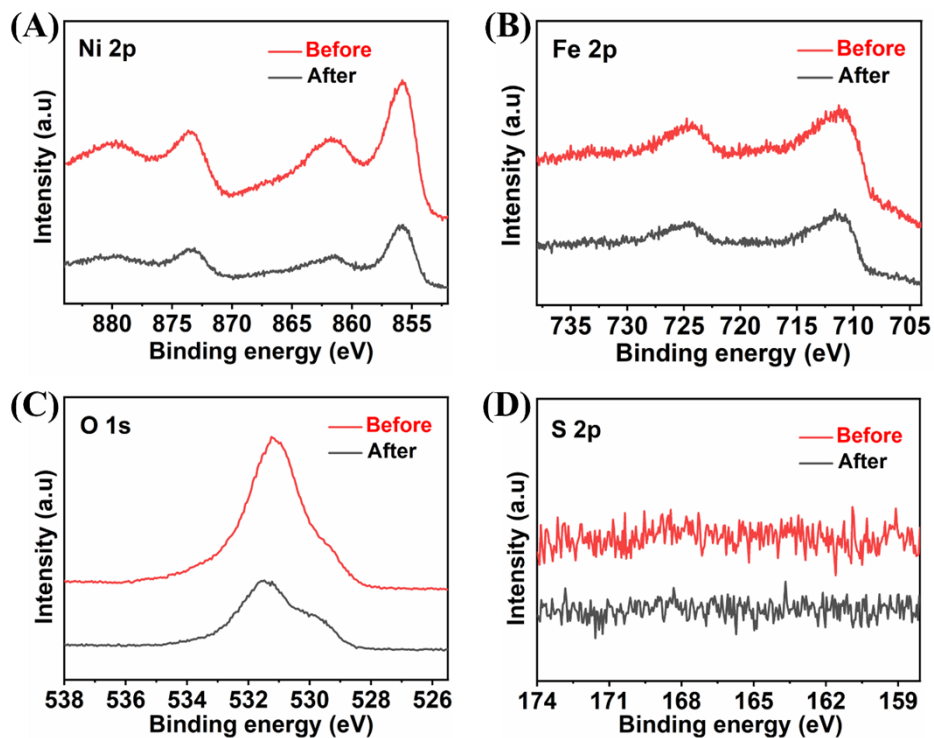


Figure S15. (A) Ni 2p, (B) Fe 2p, (C) O 1s and (D) S 2p XPS of $\text{NiFe(OH)}_x/\text{Ni}_3\text{S}_2/\text{NF}$ before and after electrolysis.

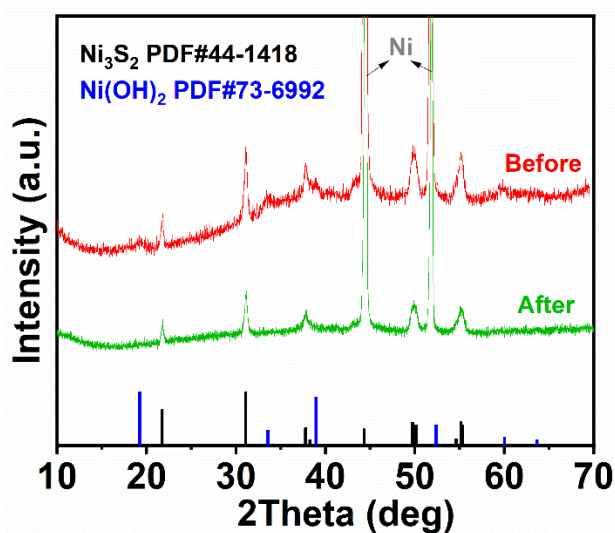


Figure S16. XRD patterns of $\text{NiFe(OH)}_x/\text{Ni}_3\text{S}_2/\text{NF}$ before and after 12 days of constant current testing.

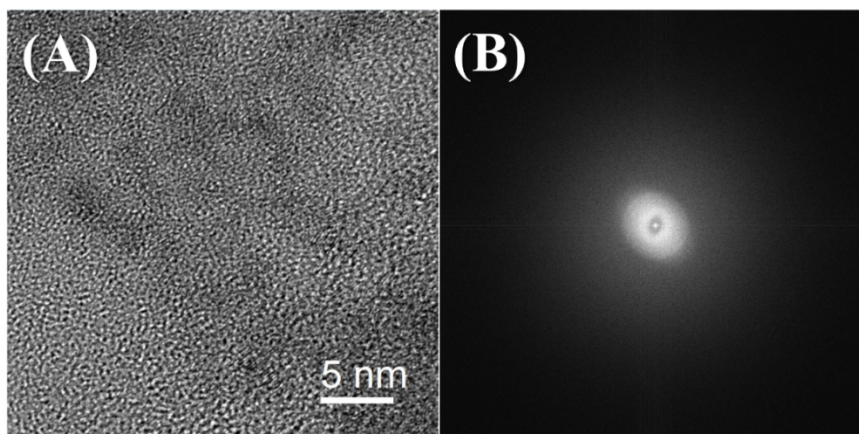


Figure S17. (A) HRTEM image and (B) Corresponding SAED pattern of $\text{NiFe(OH)}_x/\text{Ni}_3\text{S}_2$.

Table S1. Comparison of the OER performance and the methods between the $\text{NiFe(OH)}_x/\text{Ni}_3\text{S}_2/\text{NF}$ electrode and other recently reported OER electrodes in 1 M KOH electrolyte.

Catalyst	Overpotential /mV	Tafel slope (mV/dec)	Current collector	Method	Reference
$\text{NiFe(OH)}_x/\text{Ni}_3\text{S}_2/\text{NF}$	218	37.9	Ni foam	Hydrothermal/ Chemical deposition	This work
$\text{NiFe(OH)}_x/\text{Ni}_3\text{S}_2/\text{NM}$	209	55	Ni mesh	Hydrothermal	[1]
NiCe@NiFe/NF-N	254	59.9	Ni foam	Electrodeposition	[2]
CoS@NiFe LDH/NF	312	49	Ni foam	Electrodeposition	[3]
$\text{NiFe-LDH@CoS}_x/\text{NF}$	330	62	Ni foam	Hydrothermal/ Electrodeposition	[4]
$\text{NiCo}_{2-x}\text{Fe}_x\text{O}_4$	320	42	Ni foam	Electrodeposition	[5]
$\text{NiFe LDH@Ni}_3\text{N/NF}$	238	61	Ni foam	Electrodeposition	[6]
Ni@NiFe LDH	269	66.3	Ni foam	Electrodeposition	[7]
$\text{NiFe-LDH@Ni-MOF/NF}$	248	43.7	Ni foam	Hydrothermal/ Electrodeposition	[8]

References

[1] X. Wang, X. Zong, B. Liu, G. Long, A. Wang, Z. Xu, R. Song, W. Ma, H. Wang

- and C. Li, *Small* **2021**, *n/a*, 2105544.
- [2] G. Liu, M. Wang, Y. Wu, N. Li, F. Zhao, Q. Zhao and J. Li, *Applied Catalysis B: Environmental* **2020**, *260*, 118199.
- [3] Y. J. Lee and S.-K. Park, *Small* **2022**, *18*, 2200586.
- [4] Y. Yang, Y. Xie, Z. Yu, S. Guo, M. Yuan, H. Yao, Z. Liang, Y. R. Lu, T.-S. Chan, C. Li, H. Dong and S. Ma, *Chemical Engineering Journal* **2021**, *419*, 129512.
- [5] Y. Huang, S. L. Zhang, X. F. Lu, Z.-P. Wu, D. Luan and X. W. Lou, *Angewandte Chemie International Edition* **2021**, *60*, 11841-11846.
- [6] B. Wang, S. Jiao, Z. Wang, M. Lu, D. Chen, Y. Kang, G. Pang and S. Feng, *Journal of Materials Chemistry A* **2020**, *8*, 17202-17211.
- [7] Z. Cai, X. Bu, P. Wang, W. Su, R. Wei, J. C. Ho, J. Yang and X. Wang, *Journal of Materials Chemistry A* **2019**, *7*, 21722-21729.
- [8] X. Zeng, Z. Cai, C. Zhang, D. Wang, J. Xu and X. Wang, *Materials Research Letters* **2022**, *10*, 88-96.